Anal. Chem. **2010,** *82,* 8042–8046

Letters to *Analytical Chemistry*

Metal–Organic Framework Thin Film for Enhanced Localized Surface Plasmon Resonance Gas Sensing

Lauren E. Kreno, Joseph T. Hupp,* and Richard P. Van Duyne*

Department of Chemistry, Northwestern University, 2145 Sheridan Road, Evanston, Illinois 60208

Despite its high refractive index sensitivity, localized surface plasmon resonance (LSPR) spectroscopy has been generally restricted to large biological analytes. Sensing of smaller molecules is a compelling target for this technique; in particular, LSPR spectroscopy could be utilized to detect hazardous or toxic gases and manage industrial processes involving gaseous chemicals. Here, we report sensing of pure gases over Ag nanoparticles using LSPR spectroscopy, where the detected changes in bulk refractive index are $<5 \times 10^{-4}$ refractive index units (RIU). We further demonstrate a novel strategy for amplifying the sensing signal by coating the plasmonic substrate with a metal–organic framework (MOF) material. $Cu_3(BTC)_2(H_2O)_3$, BTC = benzenetricarboxylate, was grown on Ag nanoparticles using a layer-by-layer method in order to control the MOF thickness, which we show greatly affects the sensor response. Preferential concentration of CO_2 within the MOF pores produces a 14-fold signal enhancement for CO_2 sensing. In principle, MOFs can be tailored for sorbing different analytes, making them ideal materials for this amplification strategy. Because the sensing signal originates in the nanoparticle extinction spectrum and not in the MOF itself, this comprises a generalizable sensing scheme applicable to any porous MOF and any analyte.

Surface plasmon resonance spectroscopy has revolutionized optical sensing with its ability to measure extremely small changes in refractive index (RI). Schemes based on both plasmonic nanoparticles and thin films have been employed for a variety of applications including disease diagnostics,[1] food safety,[2] environmental monitoring,[3] organic vapor sensing,[4] and chemical threat detection.[5] The vast majority of this work has focused on biological sensing,[1,6–9] with the most sensitive measurements boasting detection limits below 100 protein molecules.[10] In these reports, low limits of detection (LODs) are possible due to the relatively large changes in RI associated with binding of bulky biomolecules. However, there are a limited number of reports of small molecule sensing, which is significantly more challenging due to very small changes in RI. Recent development of high-resolution instrumentation in our lab has allowed us to measure increasingly smaller changes in RI. In the quest to probe the limits of our resolution, we have demonstrated that we can even distinguish between different pure gases whose RIs vary by as little as $\sim 10^{-4}$ refractive index units (RIU).[11] Here, we report bulk sensing of small gas molecules by localized surface plasmon resonance (LSPR) spectroscopy and further demonstrate over an order of magnitude signal amplification by preconcentrating the gas molecules in a porous metal–organic framework (MOF) material grown on the sensor surface.

In LSPR spectroscopy, impinging light excites a coherent oscillation of the conduction band electrons, known as an LSPR. Absorption and scattering of light are greatly enhanced at frequencies that excite the LSPR, resulting in a characteristic extinction spectrum that depends on the size, shape, and composition of the nanoparticle as well as the RI of the external environment, *n*. Thus, changes in the dielectric environment near a nanoparticle surface can be measured as shifts in the extinction spectrum.[12]

* Corresponding authors. R.P.V.D.: e-mail, vanduyne@northwestern.edu; tel, (847) 491-3516; fax, (847) 491-7713. J.T.H.: e-mail, j-hupp@northwestern.edu; tel, (847) 491-3504.

(1) Haes, A. J.; Chang, L.; Klein, W. L.; Van Duyne, R. P. *J. Am. Chem. Soc.* **2005**, *127*, 2264–2271.
(2) Piliarik, M.; Párová, L.; Homola, J. *Biosens. Bioelectron.* **2009**, *24*, 1399–1404.
(3) Mauriz, E.; Calle, A.; Montoya, A.; Lechuga, L. M. *Talanta* **2006**, *69*, 359–364.
(4) Chen, Y.-Q.; Lu, C.-J. *Sens. Actuators, B: Chem.* **2009**, *135*, 492–498.
(5) Taranekar, P.; Baba, A.; Park, J. Y.; Fulghum, T. M.; Advincula, R. *Adv. Funct. Mater.* **2006**, *16*, 2000–2007.
(6) Haes, A. J.; Van Duyne, R. P. *J. Am. Chem. Soc.* **2002**, *124*, 10596–10604.
(7) Raschke, G.; Kowarik, S.; Franzl, T.; Sönnichsen, C.; Klar, T. A.; Feldmann, J.; Nichtl, A.; Kürzinger, K. *Nano Lett.* **2003**, *3*, 935–938.
(8) Olofsson, L.; Rindzevicius, T.; Pfeiffer, I.; Käll, M.; Höök, F. *Langmuir* **2003**, *19*, 10414–10419.
(9) Anker, J. N.; Hall, W. P.; Lyandres, O.; Shah, N. C.; Zhao, J.; Van Duyne, R. P. *Nat. Mater.* **2008**, *7*, 442–453.
(10) Dahlin, A. B.; Chen, S.; Jonsson, M. P.; Gunnarsson, L.; Käll, M.; Höök, F. *Anal. Chem.* **2009**, *81*, 6572–6580.
(11) Bingham, J. M. Ph. D. Dissertation, Northwestern University, Evanston, IL, 2010.
(12) Willets, K. A.; Van Duyne, R. P. *Annu. Rev. Phys. Chem.* **2007**, *58*, 267–297.

10.1021/ac102127p
Published on Web 09/14/2010

Gas and vapor sensing is a highly active field of research, owing to the need for sensors to detect toxic or hazardous gases, and LSPR spectroscopy has only recently been employed in this field. For example, Ag island films were used to sense volatile organic compounds in the vapor phase.[4] However, detection of smaller molecules, such as pure gases, requires high-resolution instrumentation capable of measuring very small LSPR peak shifts. We recently reported development of a low-noise LSPR spectrometer with 1.5×10^{-2} nm shift resolution.[13] For an array of triangular nanoparticles fabricated using nanosphere lithography, the theoretical limit of detectable Δn with this resolution is $\sim 7 \times 10^{-5}$ RIU (assuming a nanoparticle sensitivity factor of 200 nm/RIU, which is reasonable to attain according to previous experiments[14]). Therefore, this instrumentation is well suited to measure peak shifts induced by changes in the gaseous atmosphere where Δn is on the order of 10^{-4} RIU. Herein, we present the first direct RI-based sensing of CO_2 and SF_6 by LSPR spectroscopy using bare Ag nanoparticles. The LSPR peak shift, $\Delta\lambda_{max}$, in each gas is measured relative to the peak location, λ_{max}, in N_2. None of these gases are expected to react chemically with the nanoparticle, so the peak shift can be attributed entirely to changing the RI of the environment (rather than altering the particle itself, which has been previously reported[15]).

For practical applications, it may be necessary to detect lower concentrations of a target gas that is present as one component in a mixture, rather than as a pure gas. In the case of CO_2 sensing, our theoretical LOD using bare nanoparticles is relatively high at ~33% of CO_2 in N_2. Potential approaches to lower the LOD include increasing the sensor response via a resonant enhancement[16] or coating the particles with a material that promotes adsorption of the analyte.[4,17] The former method requires matching of the LSPR frequency with a molecular absorption, which may be impossible for analytes lacking a strong absorption in the visible or IR. In contrast, functionalizing the particles with a sorbtive coating is a generalizable strategy for amplifying the sensor response.

An ideal material for this purpose would have a high capacity for sorbing the analyte via a reversible interaction, enabling the sensor to be reused. MOFs are a promising class of materials that can satisfy these requirements. MOFs are composed of metal cation or metal cluster corners linked by multitopic organic struts, which assemble into crystalline networks.[18−20] Featuring large surface areas and permanent porosity, these structures typically show high capacity for gases and vapors.[21,22] In addition to enhancing the sensor response via concentration of the analyte, MOFs can solve another inherent drawback to a bare nanoparticle sensor: chemical nonspecificity. Using bare nanoparticles, multiple analytes may produce the same signal and, therefore, be indistinguishable; preferential adsorption of the analyte by a sorbent on the nanoparticle surface could exclude interfering agents. Previously, others have improved LSPR vapor selectivity using self-assembled monolayers (SAMs)[4] and polymers.[17] However, these schemes simply rely on association of molecules with similar polarity, interactions which are not highly specific and would not be applicable to gas sensing. In contrast, both pore size and chemical functionality of MOFs can be controlled through choice of precursors and synthetic conditions, yielding tunable chemical selectivity based on molecular sieving effects, $\pi-\pi$ stacking, hydrogen bonding, electrostatic interactions, etc. The ability to rationally design structures allows MOF sorption properties to be tailored for gas separation,[23] storage,[24] catalysis,[25] and sensing.[26−28] In principle, the myriad combinations of metal cations and linker molecules offer an essentially endless pool of possible MOF structures, making the synthetic variability a significant advantage of our plasmonic MOF sensor.

Here, we apply this signal amplification principle to CO_2 sensing with our Ag nanoparticle sensor using a prototypical MOF, $Cu_3(BTC)_2(H_2O)_3$ (HKUST-1). Composed of paddlewheel-type Cu^{2+} nodes linked with benzenetricarboxylate (BTC),[29] HKUST-1 is one of the most widely studied and well-characterized MOFs.[30−32] Furthermore, its CO_2 sorption properties[33] and synthesis on metal surfaces[34,35] have been previously documented, making it an ideal test material. By growing HKUST-1 on the surface of our Ag nanoparticle sensor, we demonstrate a 14-fold enhancement of the CO_2 sensing signal via selective concentration of CO_2 in the MOF pores. The sensor response depends on the thickness of the MOF film and can be calibrated to detect lower concentrations of CO_2 in N_2. In addition to providing a means of amplifying LSPR response, this work presents a novel approach to MOF sensing. The vast majority of existing literature relies on photolumines-

(13) Hall, W. P.; Anker, J. N.; Lin, Y.; Modica, J.; Mrksich, M.; Van Duyne, R. P. *J. Am. Chem. Soc.* **2008**, *130*, 5836–5837.
(14) Jensen, T. R.; Duval, M. L.; Kelly, K. L.; Lazarides, A. A.; Schatz, G. C.; Van Duyne, R. P. *J. Phys. Chem. B* **1999**, *103*, 9846–9853.
(15) Larsson, E. M.; Edvardsson, M. E. M.; Langhammer, C.; Zoric, I.; Kasemo, B. *Rev. Sci. Instrum.* **2009**, *80*, 125105–125110.
(16) Herminjard, S.; Sirigu, L.; Herzig, H. P.; Studemann, E.; Crottini, A.; Pellaux, J.-P.; Gresch, T.; Fischer, M.; Faist, J. *Opt. Express* **2009**, *17*, 293–303.
(17) Karakouz, T.; Vaskevich, A.; Rubinstein, I. *J. Phys. Chem. B* **2008**, *112*, 14530–14538.
(18) Kitagawa, S.; Kitaura, R.; Noro, S. *Angew. Chem., Int. Ed.* **2004**, *43*, 2334–2375.
(19) Férey, G. *Chem. Soc. Rev.* **2008**, *37*, 191–214.
(20) Tranchemontagne, D. J.; Mendoza-Cortes, J. L.; O'Keeffe, M.; Yaghi, O. M. *Chem. Soc. Rev.* **2009**, *38*, 1257–1283.
(21) Sun, D.; Ma, S.; Ke, Y.; Collins, D. J.; Zhou, H.-C. *J. Am. Chem. Soc.* **2006**, *128*, 3896–3897.
(22) Cychosz, K. A.; Wong-foy, A. G.; Matzger, A. J. *J. Am. Chem. Soc.* **2008**, *130*, 6938–6939.
(23) Li, J.-R.; Kuppler, R. J.; Zhou, H.-C. *Chem. Soc. Rev.* **2009**, *38*, 1477–1504.
(24) Collins, D. J.; Zhou, H.-C. *J. Mater. Chem.* **2007**, *17*, 3154–3160.
(25) Lee, J.; Farha, O. K.; Roberts, J.; Scheidt, K. A.; Nguyen, S. T.; Hupp, J. T. *Chem. Soc. Rev.* **2009**, *38*, 1450–1459.
(26) Allendorf, M. D.; Houk, R. J. T.; Andruszkiewicz, L.; Talin, A. A.; Pikarsky, J.; Choudhury, A.; Gall, K. A.; Hesketh, P. J. *J. Am. Chem. Soc.* **2008**, *130*, 14404–14405.
(27) Chen, B. L.; Wang, L. B.; Xiao, Y. Q.; Fronczek, F. R.; Xue, M.; Cui, Y. J.; Qian, G. D. *Angew. Chem., Int. Ed.* **2009**, *48*, 500–503.
(28) Lu, G.; Hupp, J. T. *J. Am. Chem. Soc.* **2010**, *132*, 7832–7833.
(29) Chui, S. S. Y.; Lo, S. M. F.; Charmant, J. P. H.; Orpen, A. G.; Williams, I. D. *Science* **1999**, *283*, 1148–1150.
(30) Schlichte, K.; Kratzke, T.; Kaskel, S. *Microporous Mesoporous Mater.* **2004**, *73*, 81–88.
(31) Prestipino, C.; Regli, L.; Vitillo, J. G.; Bonino, F.; Damin, A.; Lamberti, C.; Zecchina, A.; Solari, P. L.; Kongshaug, K. O.; Bordiga, S. *Chem. Mater.* **2006**, *18*, 1337–1346.
(32) John, N. S.; Scherb, C.; Shoaee, M.; Anderson, M. W.; Attfield, M. P.; Bein, T. *Chem. Commun.* **2009**, 6294–6296.
(33) Yazaydin, A. O.; Benin, A. I.; Faheem, S. A.; Jakubczak, P.; Low, J. J.; Willis, R. R.; Snurr, R. Q. *Chem. Mater.* **2009**, *21*, 1425–1430.
(34) Biemmi, E.; Scherb, C.; Bein, T. *J. Am. Chem. Soc.* **2007**, *129*, 8054–8055.
(35) Shekhah, O.; Wang, H.; Kowarik, S.; Schreiber, F.; Paulus, M.; Tolan, M.; Sternemann, C.; Evers, F.; Zacher, D.; Fischer, R. A.; Wöll, C. *J. Am. Chem. Soc.* **2007**, *129*, 15118–15119.

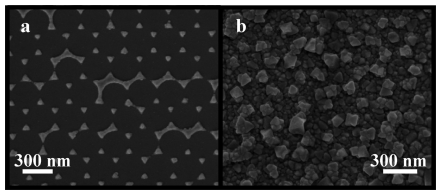

Figure 1. SEM images of (a) a triangular Ag nanoparticle array fabricated by nanosphere lithography on a glass coverslip and (b) a Ag nanoparticle array coated with 20 cycles of polycrystalline HKUST-1 film.

cent MOF structures.[36,37] In contrast, our sensor architecture is not MOF-specific and, therefore, can be broadly applied to a range of MOF materials for future studies.

EXPERIMENTAL SECTION

Fabrication of Plasmonic Substrates. Arrays of Ag nanoparticles were fabricated according to reported methods using nanosphere lithography.[38] Briefly, 40 nm of silver metal was thermally evaporated over a monolayer of 290 or 390 nm diameter polystyrene spheres (Thermo Scientific) on a round glass microscope coverslip. Removal of the spheres by tape stripping and sonication produced arrays of triangular nanoparticles.

Growth of HKUST-1 on Nanoparticles. HKUST-1 was grown using a layer-by-layer method as reported by Shekhah et al.[35] Nanoparticle arrays were first soaked in a 1 mM solution of 11-mercaptoundecanoic acid (Aldrich) in ethanol for 24 h to form a SAM. Subsequently, HKUST-1 was grown in cycles, where one cycle consisted of subsequent immersions in 1 mM ethanol solutions of copper(II) acetate and benzenetricarboxylic acid (Aldrich). This procedure was repeated with rinsing and drying between each immersion.

Characterization and Sensing Experiments. MOF/nanoparticle composites (MOF/NP) were characterized using grazing-incidence X-ray diffraction (Rigaku ATX-G) and scanning electron microscopy (LEO Gemini 1525, SEM). A new generation of our high-resolution LSPR spectrometer was designed for these experiments, incorporating the ability to dose gases to the surface in a highly controlled manner and subsequently monitor the gas composition by mass spectrometry. Extinction spectra were collected in a transmission geometry and the peak extinction was monitored in real-time. A detailed explanation of the experimental setup can be found in the Supporting Information.

RESULTS AND DISCUSSION

Gas sensing experiments were first performed with nonfunctionalized Ag nanoparticle arrays (Figure 1a). Prior to each experiment, the sample was purged overnight with dry N_2. Then, a test gas (CO_2 or SF_6) was dosed in 60 s pulses, separated by 60 s pulses of N_2. When the test gas was switched on, N_2 was simultaneously switched off, such that only one gas flowed over the sample at a time. Figure 2a shows the sensor response to both test gases for five repeated pulses. When the test gas was introduced (at $t = 30$ s), a red shift was observed as an increase in $\Delta\lambda_{max}$. This corresponds to the higher refractive indices of CO_2 and SF_6 (1.000449 RIU and 1.000703 RIU, respectively) relative to N_2 (1.000298 RIU). Upon purging the sample cell with N_2, the LSPR peak blue-shifted back to its baseline value. For each test gas, ten repeated pulses were analyzed for the variation in $\Delta\lambda_{max}$ to determine reproducibility. In general, the standard deviation in the peak shift was less than the noise in λ_{max} itself (0.003 nm), indicating that our results are highly consistent in repeated uses of the sensor.

Without functionalization of the nanoparticle surface, we do not expect any interaction of the analyte with the sensor. Therefore, $\Delta\lambda_{max}$ should scale with $\Delta n = n_{testgas} - n_{N_2}$. In agreement with this prediction, we do observe a larger $\Delta\lambda_{max}$ for SF_6 than CO_2 (0.17 nm vs 0.13 nm). However, the ratio of the responses is not what we expect; $\Delta\lambda_{max}$ (SF_6): $\Delta\lambda_{max}$ (CO_2) should be ~2.7, whereas we measure a ratio of ~1.3. One possible explanation for this discrepancy is adsorption of gas molecules on the surface of the nanoparticle, yielding an effective n greater than that of the bulk gas. Surface adsorption seems probable since the magnitude of our observed $\Delta\lambda_{max}$ is ~2−4 times larger than expected. We suspect that the major contribution to this apparent adsorption is actually trace water vapor from the gas supplies. Care is taken to exclude as much water as possible using dry, high purity gases coupled with inline moisture traps, but mass spectrometry measurements (not published here) indicate that the CO_2 and SF_6 contain slightly higher amounts of trace water than the N_2 purge gas. Furthermore, we observe unexpectedly large responses for both CO_2 and SF_6 but have found no literature precedent for adsorption of SF_6 on Ag surfaces at room temperature. Importantly, we can still resolve the difference between CO_2 and SF_6, which is especially discernible in the fast bulk response that occurs within the first few seconds following gas switching. This possible contaminant interference, evidenced by the slower rise in λ_{max} following the initial jump, only underscores the need for a selective sorbent coating on the sensor.

As mentioned previously, it is also necessary to improve the LOD of this measurement for practical applications. We synthesized the MOF HKUST-1 on the nanoparticle surface to improve the LOD and chemical selectivity of our sensor via selective preconcentration of our analyte. Figure 1b shows an SEM image of a Ag nanoparticle array coated with 20 cycles of HKUST-1. The MOF film appears highly crystalline and forms a dense coating over both the metal and glass surfaces. Larger crystallites follow the pattern of the underlying nanoparticle array, implying that the −COOH terminated SAM templates the growth of large HKUST-1 crystals. In contrast, smaller crystallites grow on the bare glass surface. While the SAM is not expected to form on the glass, the coverslip substrate is initially treated with a basic solution to promote electrostatic self-assembly of the polystyrene nanospheres. Thus, −OH groups are likely present on the glass surface, providing nucleation sites for MOF crystallization, as has been reported on −OH terminated SAMs.[34] Comparison of the X-ray diffraction patterns of the MOF/NP with bulk HKUST-1 powder confirmed that the correct crystalline phase was formed (Figure S4, Supporting Information).

(36) Chen, B.; Yang, Y.; Zapata, F.; Lin, G.; Qian, G.; Lobkovsky, E. B. *Adv. Mater.* **2007**, *19*, 1693–1696.
(37) Wong, K. L.; Law, G. L.; Yang, Y. Y.; Wong, W. T. *Adv. Mater.* **2006**, *18*, 1051–1054.
(38) Haynes, C. L.; Van Duyne, R. P. *J. Phys. Chem. B* **2001**, *105*, 5599–5611.

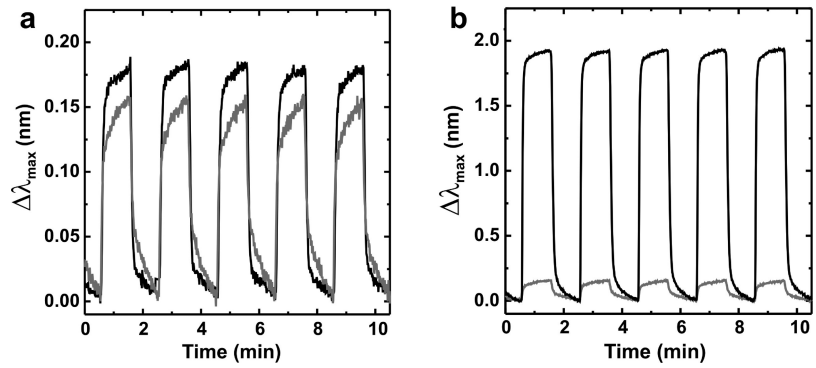

Figure 2. (a) Response of a bare Ag nanoparticle sensor to pure SF_6 (black) and pure CO_2 (gray) and (b) comparison of bare nanoparticle sensor (gray) and MOF-coated sensor (black) responses to CO_2. In both cases, the sample starts in N_2 atmosphere and the test gas is dosed at $t = 30$ s. After an additional 60 s, the sample is purged with N_2 and this cycle is repeated five times.

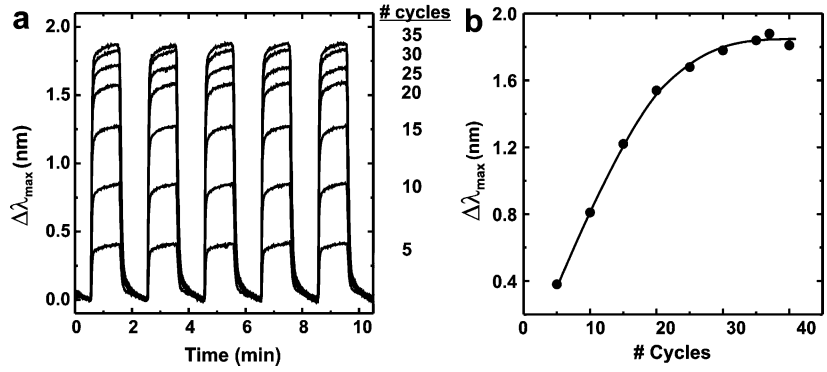

Figure 3. (a) Sensor response to CO_2 for increasing numbers of HKUST-1 growth cycles. (b) Average $\Delta\lambda_{max}$ as a function of number of growth cycles (solid line provided to guide the eye); $\Delta\lambda_{max}$ increases rapidly as a function of MOF thickness at low numbers of growth cycles and tapers off as MOF thickness presumably approaches the total sensing volume, reaching a maximum $\Delta\lambda_{max}$ of 1.88 nm at 37 growth cycles.

To probe the effect of the MOF film, the CO_2 sensing procedure was repeated for Ag particles functionalized with HKUST-1. Several different outcomes are possible when the MOF sorbs an analyte which may give rise to competing effects in terms of the LSPR peak shift. The most intuitive result is an increase in the MOF RI when formerly vacant pores are filled with analyte. This increase in RI would result in a red shift of the nanoparticle plasmon resonance. If the pores are not vacant but rather the analyte displaces guest molecules in the pores, then a red or blue shift might be observed on the basis of the corresponding RIs and the MOF sorption capacity for those molecules. Last, the MOF structure could slightly expand or contract upon sorption of an analyte. For example, HKUST-1 is known to expand by 0.45% of its size upon hydration.[26] This lattice expansion would result in a blue shift of a plasmonic sensor. In our sensor, these three effects probably all contribute to the LSPR peak shift; ultimately, we observe a red shift upon adsorption of CO_2. Figure 2b shows results for the MOF/NP sample with the maximum response to CO_2 overlaid with the same experiment using bare nanoparticles. In the bare particle case, $\Delta\lambda_{max} = 0.13$ nm. The sensor coated with 37 cycles of KHUST-1 exhibits $\Delta\lambda_{max} = 1.88$ nm, a 14-fold larger signal. This significant signal enhancement is not surprising, as HKUST-1 readily sorbs larger amounts of CO_2 than N_2. At our operating pressure (~1 atm), the MOF may adsorb almost 10 times more CO_2 than N_2, according to reported isotherms.[39]

To further corroborate our hypothesis that the MOF is selectively concentrating CO_2, we studied the dependence of the signal enhancement on MOF film thickness. As shown in Figure 3a, $\Delta\lambda_{max}$ increases with increasing number of MOF growth cycles. As the free space around the nanoparticle is filled with MOF, we expect more CO_2 to be concentrated within the sensing volume, producing an increase in $\Delta\lambda_{max}$. The plasmon-induced electromagnetic field decays exponentially from the nanoparticle surface, so molecules closest to the nanoparticle have the greatest effect on $\Delta\lambda_{max}$. Thus, we expect $\Delta\lambda_{max}$ to increase rapidly at low numbers of growth cycles, when new MOF growth is closest to the surface, and subsequently taper off as it approaches the maximum. Figure 3b shows that our observation is in good agreement with this prediction. The MOF/NP sensor did not show enhanced signals for SF_6 sensing. In contrast, it displayed the opposite trend, where $\Delta\lambda_{max}$ decreased with increasing MOF thickness, implying that the HKUST-1 film exhibits negligible SF_6 sorption (data not shown).

The dynamic range of the sensor was studied by measuring $\Delta\lambda_{max}$ as a function of CO_2 concentration. A range of concentrations was achieved by mixing the pure N_2 and CO_2 streams.

(39) Chowdhury, P.; Bikkina, C.; Meister, D.; Dreisbach, F.; Gumma, S. *Microporous Mesoporous Mater.* **2009**, *117*, 406–413.

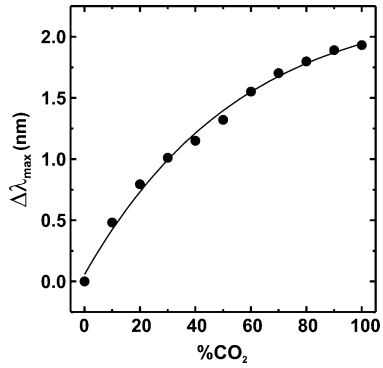

Figure 4. MOF/NP sensor response as a function of CO_2 concentration in N_2. Solid line is provided as a guide to the eye.

The percentage of CO_2 was increased in 10% increments, keeping the total flow rate of the dosing stream constant. From the resulting data, we can gain some insight into the hydration state of the MOF by comparison with reported adsorption isotherms of dehydrated, partially, and fully hydrated HKUST-1 powders. A plot of $\Delta\lambda_{max}$ vs % CO_2 (Figure 4) resembles the shape of the CO_2 adsorption isotherm of a partially hydrated HKUST-1 sample.[33] We expect that purging the sample with N_2 overnight for our experiment removes the majority of noncoordinated solvent molecules. However, some solvent likely remains bound to Cu^{2+} sites because the sample is not evacuated at low pressure. These data further suggest that CO_2 concentrations well below 10% (the lowest measured concentration) could be detected. Most importantly, these results demonstrate a method for calibration of our sensor which would allow us to extrapolate an unknown concentration of CO_2 by measuring $\Delta\lambda_{max}$.

CONCLUSIONS

We have demonstrated direct sensing of pure SF_6 and CO_2 by measuring changes in bulk RI using LSPR spectroscopy without the need for signal enhancement. Measurement of these small Δns was made possible using a high-resolution UV−vis transmission spectrometer which tracks LSPR peak position with a typical noise level ~0.003 nm. Furthermore, we have demonstrated the ability of a MOF to "recruit" molecules to the sensing surface, enhancing our signal by over an order of magnitude. Not only can the MOF act as a molecular sponge to increase the concentration of the analyte, but also it provides selectivity, favoring a desired analyte over other molecules present in the atmosphere. This results in increases in both sensing signal and sensor selectivity as compared to nonfunctionalized nanoparticles, which are not expected to exhibit selectivity. The layer-by-layer method of MOF growth yields excellent control over MOF thickness which we have shown to have a significant influence on sensor response.

While HKUST-1 is not known for exceptional selectivity, we expect that the overall LOD can be improved for future applications by choosing MOFs which are more selective and have high sorption capacities for a desired analyte. For example, we have demonstrated that ZIF-8 is selective for sensing nonpolar molecules due to its hydrophobic pores.[28] Other attractive candidates are metalloporphryin-containing MOFs, which should be selective based on axial ligation of guest molecules by the metal center. Our lab has reported a porphyrin MOF with guest-accessible Zn^{2+} sites which preferentially bind imine functionalities.[40] We are currently working to establish methods for synthesizing these types of MOF materials on the surface of our plasmonic sensor.

Overall, this work presents a unique coupling of a highly porous crystalline sorbent with exceptionally sensitive LSPR spectroscopy. Separately, neither the plasmonic nanoparticle array nor the MOF functions as a practical sensor, the former due to its chemical nonspecificity and the latter because it lacks a means of signal transduction. However, combining these features provides a generalizable strategy applicable, in principle, to any porous MOF and any analyte.

ACKNOWLEDGMENT

This work was supported by the Defense Threat Reduction Agency (HDTRA 1-09-1-0007), the Northwestern NSEC (NSF EEC-0647560), and the Department of Defense through an NDSEG fellowship (L.E.K.). We thank Dr. Jeffrey Anker and Dr. Julia Bingham for preliminary LSPR gas sensing measurements.

SUPPORTING INFORMATION AVAILABLE

Detailed description, schematic, and photograph of experimental setup as well as characterization of samples by X-ray diffraction. This material is available free of charge via the Internet at http://pubs.acs.org.

Received for review August 12, 2010. Accepted September 8, 2010.

AC102127P

(40) Shultz, A. M.; Farha, O. K.; Hupp, J. T.; Nguyen, S. T. *J. Am. Chem. Soc.* **2009**, *131*, 4204–4205.